Coupled Nonpolar-Polar Metal-Insulator Transition in 1:1 SrCrO_{3}/SrTiO_{3} Superlattices: A First-Principles Study

Yuanjun Zhou and Karin M. Rabe

Phys. Rev. Lett. **115**, 106401 — Published 31 August 2015

DOI: 10.1103/PhysRevLett.115.106401

Coupled nonpolar-polar metal-insulator transition in 1:1 $SrCrO_3/SrTiO_3$ superlattices: A first-principles study

Yuanjun Zhou and Karin M. Rabe
Rutgers, the State University of New Jersey
(Dated: August 10, 2015)

Using first principles calculations, we determined the epitaxial-strain dependence of the ground state of the 1:1 $SrCrO_3/SrTiO_3$ superlattice. The superlattice layering leads to significant changes in the electronic states near the Fermi level, derived from Cr t_{2g} orbitals. An insulating phase is found when the tensile strain is greater than 2.2% relative to unstrained cubic $SrTiO_3$. The insulating character is shown to arise from Cr t_{2g} orbital ordering, which is produced by an in-plane polar distortion that couples to the superlattice d-bands and is stabilized by epitaxial strain. This effect can be used to engineer the band structure near the Fermi level in transition metal oxide superlattices.

PACS numbers: 75.70.Cn, 75.80.+q, 63.20.-e, 75.10.Hk

Metal-insulator transitions (MIT) occur in many transition metal oxides as a function of composition, temperature, pressure and epitaxial strain [1]. At the atomic scale, the mechanism for the metal-insulator transition depends on the physics of the insulating state. For Mott insulators, the relevant parameters are the transition metal (TM) d-level occupation, which can be changed through doping, and the bandwidth, which can be changed by varying the TM-oxygen-TM bond angles. For band insulators, a gap can be opened at the Fermi level by a structural distortion that lowers the crystal symmetry. A symmetry-breaking distortion that lifts the degeneracy of a partially occupied state will always lower the energy; this is called a Jahn-Teller (JT) distortion[2, 3] or a Peierls distortion depending on whether the degenerate states are localized atomic orbitals or extended bands. Polar distortions have also been shown to couple to states near the Fermi level, proving useful in band-gap engineering[4, 5]. When the distortion can be controlled by an applied field or stress, the system can dynamically be driven back and forth through the MIT, a property of particular interest for applications to high-performance switching devices[6, 7],

$SrCrO_3$ (SCO) is a d^2 perovskite. It was initially reported as a paramagnetic and metallic cubic perovskite[8]. Experimental studies also showed a tetragonal C type antiferromagnetic (C-AFM) phase, with the Neel temperature below 100K and space group $P4/mmm$, coexisting with the cubic phase at low temperature[9, 10]. This tetragonal C-AFM state has been further investigated in first-principles studies[11, 12]. It exhibits a partial orbital ordering d^1_{xy},$(d_{yz}d_{xz})^1$, where the d_{xy} is nearly occupied while d_{yz} and d_{xz} orbitals are both half occupied[10, 11]. For the single-unit-cell film of SCO epitaxially grown on $SrTiO_3$, due to the missing apical oxygen of the Cr-centered oxygen octahedron at the surface, d_{yz} and d_{xz} orbitals become lower in energy than d_{xy}, leading to a $d^1_{yz}d^1_{xz}d^0_{xy}$ orbital ordering and an insulating state[13]. However, recently Zhou *et al* claimed that SCO is an insulator while the insulator-metal transition occurs under sufficient pressure[14], due to the bond instability found around 4 GPa; this suggests strong coupling between structure and electronic structure.

Layering a d-band perovskite oxide in a superlattice with a d^0 insulating perovskite will lead to large changes in the d-band states near the Fermi level, depending on the thickness of the d-band layer [15–17]. $SrTiO_3$ (STO) is a natural choice as the second component. It is a d^0 insulator with a 3.25 eV band gap and an A-site cation in common with SCO. In addition, the structure of STO can be tuned by epitaxial strain, with different octahedral rotation patterns and polar distortions in compressive and tensile strain[18–20]; these distortions are expected to influence the structure in the SCO layer.

In this Letter, we present first-principles results for the ground-state phase sequence of the 1:1 $SrCrO_3/SrTiO_3$ superlattice with varying epitaxial strain, with a first-order MIT from a metallic x-type $P2_1/c$ phase to a polar insulating G-type $Pmm2$ phase observed at 2.2% tensile epitaxial strain. We show that the insulating character arises from orbital ordering induced by a polar distortion in the SCO layer. The polar distortion is shown to be stabilized by a combination of epitaxial strain and the polar distortion in the adjacent STO layer. This offers the possibility of driving the system through the MIT by an applied field or stress that coupled to the polar mode.

Our first-principles calculations were performed using the local density approximation[21, 22] with Hubbard U (LDA+U) method implemented in the *Vienna Ab initio Simulation Package* (VASP-5.2[23, 24]). We used the Dudarev implementation[25] with effective on-site Coulomb interaction $U = 1.5$ eV to describe the localized $3d$ electron states of Cr atoms[26, 27]. The projector augmented wave (PAW) potentials[28, 29] contain 10 valence electrons for Sr ($4s^24p^65s^2$), 12 for Cr ($3p^63d^44s^2$), 10 for Ti ($3p^63d^24s^2$) and 6 for O ($2s^22p^4$). $\sqrt{2} \times \sqrt{2} \times 2$ and $2 \times 2 \times 2$ cells were used to accommodate the struc-

tural distortions and magnetic orderings considered for the 1:1 superlattice. 500 eV energy cutoff, $4 \times 4 \times 4$ k mesh and 5×10^{-3} eV/Å force threshold were used for structural relaxations. A $15 \times 15 \times 11$ k-point mesh was used for density of states calculations. Our calculations give $a = 3.812$Å for the relaxed tetragonal state of C-AFM $SrCrO_3$, consistent with the previous first-principles and experimental studies[10, 11], with aspect ratio $c/a = 0.964$ slightly smaller than the experimental value of 0.99. The epitaxial strain value is defined with respect to 3.849Å, the computed lattice constant of cubic STO. The effects of epitaxial strain were studied through "strained bulk" calculations[30].

At each value of epitaxial strain in the range -4% - 3%, we determined the ground state (GS) structure of the superlattice using the "stacking method" [20]. This method is based on the assumption that for the GS structure of the superlattice, structures of the constituent layers derive from a low-energy state of the pure compound at the relevant epitaxial strain. This therefore involved determining the low energy structures of epitaxially strained SCO and STO, as described in the supplementary material[31], and combining them to obtain a set of starting structures, which were then relaxed to the nearest energy minimum using first-principles calculations.

For the 1:1 superlattice, we consider three simple magnetic orderings for the moments of the Cr in the CrO_2 plane for each starting structure. As shown in Fig. 1(a), the three orderings are ferromagnetic (F), checkerboard ordering (G), and x-type AFM, combining AF ordering along x with ferromagnetic ordering along y. The x-type ordering is the single-layer analogue of the C-AFM ordering in the bulk ground state of $SrCrO_3$. To complete the application of the stacking method, we carried out relaxations for a small number of random starting structures[20]. These showed that from -3% to -1% epitaxial strain, the JT distortion is found in the SCO layer for G and x magnetic ordering, though in this range of epitaxial strain it does not lower the energy of the pure compound.

In Fig.1(b) we plot the epitaxial strain dependence of the total energies of the GS of the superlattice for each of the three magnetic orderings. From -3% to 2.2%, the x-AFM is the GS magnetic ordering. Above 2.2%, the GS magnetic ordering is G-AFM. It is noteworthy that while the energy differences among magnetic orderings are relatively large for compressive strain, they become close to zero for tensile strain. In particular, for tensile strain in the range of 1% – 2%, the superlattice may be paramagnetic down to low temperatures.

We summarize the epitaxially-strained lowest-energy structure and distortion patterns for each magnetic ordering in Fig. 1(c). There are several features that worth noting. As the epitaxial strain goes from compressive to tensile, the out-of-plane rotation $a^0a^0c^-$ is suppressed,

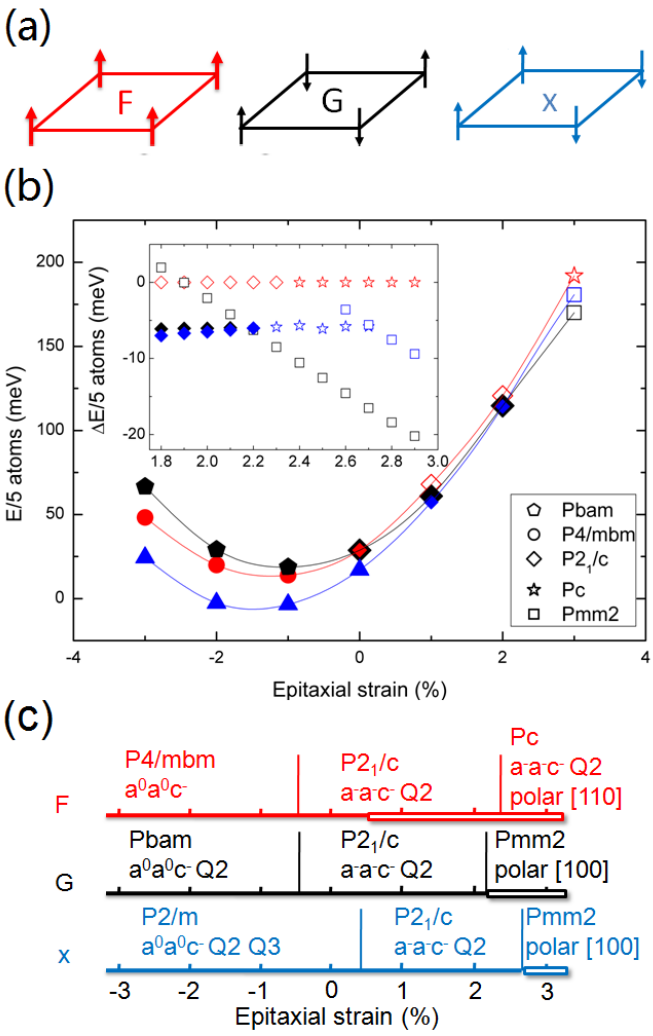

FIG. 1. (a) Magnetic orderings for the CrO_2 layer of the SCO/STO superlattice. Red: ferromagnetic (F), black: G-AFM (G), and blue: x-type AFM (x) states. (b) Lowest energy structures and energies for F (red), G (black), and x (blue) magnetic orderings as functions of epitaxial strain. The solid curves guide the eye. Insulating and metallic states are denoted by open and solid symbols. Shapes of data points indicate the space groups. The inset shows the energies of low energy structures relevant to the F state in the epitaxial strain range 1.8% to 2.9%. (c) Lowest energy and epitaxially strained structures summarized from (b). Solid and hollow lines represent metallic and insulating phases, respectively. We use Glazer notation [35] to denote the octahedral rotations. JT Q_2 and Q_3 modes have been defined previously [2, 3].

while in-plane rotations $a^-a^-c^0$ become more favorable. Amplitudes of JT distortions in the SCO layer are about 1% of the lattice constant, and roughly independent of epitaxial strain. In-plane polar distortions appear for tensile epitaxial strain and are characteristic of insulating states. Computation of the dependence of the energy as a function of the amplitude of the polar mode in this

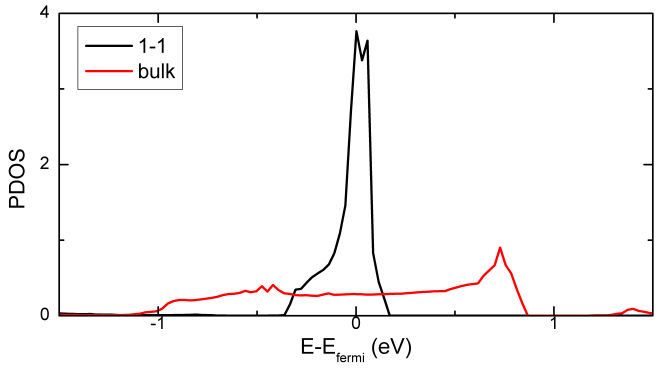

FIG. 2. The PDOS of the Cr d_{yz} orbital in the G-type 1:1 SCO/STO superlattice and in C-type bulk SCO, both at 3% tensile strain in the high-symmetry P4mm structure

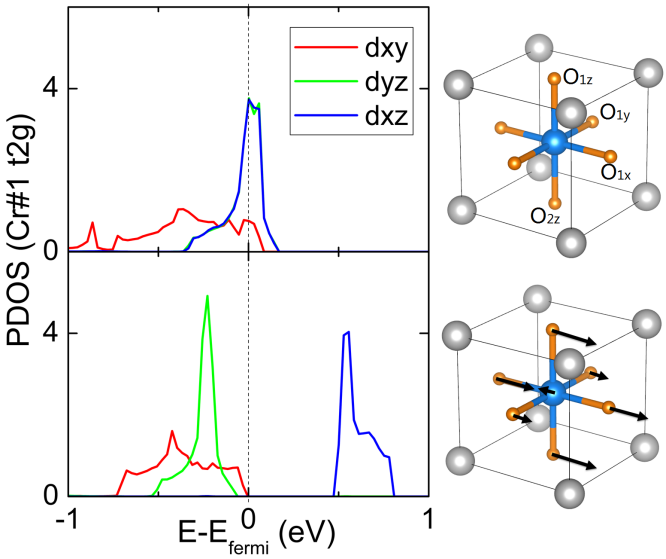

FIG. 3. PDOS of the spin up Cr t_{2g} in the 1:1 superlattice for +3% strain, with G-AFM magnetic ordering. The left panels represent the PDOS without (top) and with (bottom) the polar distortion. The vertical dashed line marks the energy of the highest occupied state. The distortions in the SCO layer are shown on the right part, where gray, blue and orange spheres represent Sr, Cr and O ions, respectively.

strain range, shown in the supplementary material, reveals a cusp, with linear dependence for small distortion amplitudes. This is related to orbital ordering and the coupling of this distortion to the d states of Cr, as will be discussed further below.

The phase boundary at 2.2% epitaxial strain is of particular interest. At this epitaxial strain, there is a metal-insulator transition from the x-type nonpolar $P2_1/c$ state to the G-type polar $Pmm2$ state. A close-up picture of the transition can be obtained from the inset of Fig. 1, which shows the energies for relaxed lowest energy F, G, and x structures for 1.8% – 2.9% epitaxial strain. With increasing epitaxial strain, the energy of the G-AFM polar $Pmm2$ structure decreases relative to that of the x-type nonpolar $P2_1/c$ structure, with a first-order transition at 2.2% epitaxial strain.

To figure out the mechanism of the insulating phase in the 1:1 superlattice beyond 2.2% epitaxial strain, we first consider the effect of the superlattice layering on the bands near the Fermi level. In Fig. 2, we show the PDOS of d_{yz} of one Cr atom in the G-type 1:1 superlattice and C-AFM bulk SCO for 3% tensile epitaxial strain in the $P4/mmm$ symmetry. The 1:1 superlattice is metallic for the $P4/mmm$ structure, with the d_{yz} band much narrower than in the bulk case. The effect of layering is thus to eliminate the dispersion of the Cr t_{2g} bands along k_z, and significantly to narrow the band widths of d_{yz} and d_{xz}. The thickness of the STO layer has in contrast seen to have little effect, our calculations showing that the Cr-layer structure and bands are very similar for 1:1 and 1:3 superlattices.

Next, we consider the coupling effect of the polar distortion to the superlattice insulating $Pmm2$ state. The $Pmm2$ structure is generated from the high symmetry reference structure by the doubly-degenerate in-plane E_u polar distortion, with eigenvector (0.00, 0.00, −0.15, 0.08, 0.53, 0.53, 0.37, 0.40, 0.06, 0.33) specifying the displacement pattern of the atoms (Sr, Sr, Cr, Ti, O_{z1}, O_{z2}, O_{x1}, O_{x2}, O_{y1}, O_{y2}). From 2.2% to 3%, the band gap increases from 0.27 to 0.47 eV, and the polarization increases from 36 to 41 $\mu C/cm^2$.

The effects of the in-plane polar distortion on the electronic structure of the superlattice are evident from the projected density of states (PDOS) of the t_{2g} bands of the spin up Cr atom, shown in Fig. 3. The layered structure of the superlattice splits d_{xy} from d_{xz} and d_{yz} and increasing tensile epitaxial strain lowers the energy of the d_{xy} orbital relative to d_{yz} and d_{xz}. At 3% epitaxial strain, in the undistorted structure, all three d orbitals are partially occupied. The in-plane polar distortion lifts the degeneracy of d_{yz} and d_{xz}, so that in the polar $Pmm2$ state the d_{xy} and d_{yz} orbitals are fully occupied while d_{xz} is unoccupied, corresponding to $d^1_{xy}d^1_{yz}d^0_{xz}$ orbital ordering.

In fact, the orbital ordering can be produced by polar displacements just of the Cr atoms. To show this, we consider a $Pmm2$ 1:1 SCO/STO superlattice, in which only the Cr atoms are uniformly displaced along [100], while all other atoms stay at the high symmetry positions. In Fig. 4 we show the PDOS of the distorted superlattice as a function of Cr displacement. There is a dramatic downward shift of the d_{yz} with increasing displacement, accompanied by a smaller upward shift of d_{xy} and a decrease in the d_{xy} bandwidth.

Finally, we discuss why the in-plane polar distortion

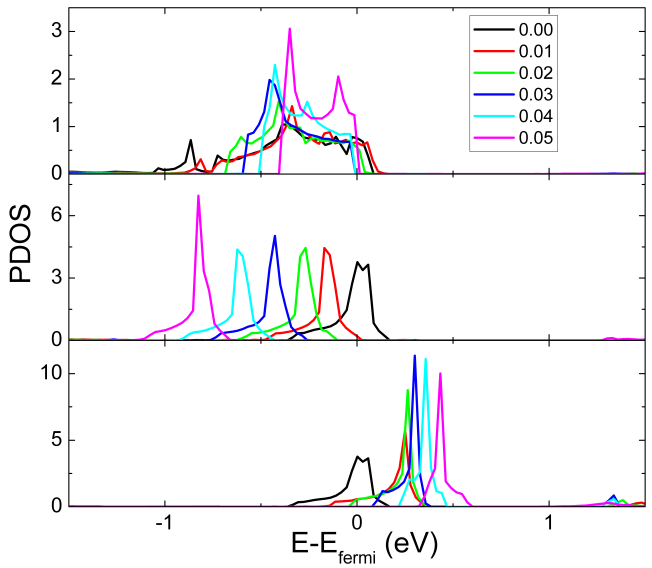

FIG. 4. The evolution of PDOS of Cr d_{xy}, d_{yz} and d_{xz} as a function of polar displacement of Cr ion in [100]. The amplitude of the displacement for each curve is given in the legend in units of the in-plane lattice constant.

becomes the GS for tensile strain. Our calculations show that for any distortion that lifts the d_{yz} and d_{xz} degeneracy, there is a linear energy gain. This explains the emergence of JT distortions in $P2_1/c$ or $Pbam$ structures for the 1:1 superlattice. However, in general, for large tensile epitaxial strain, the in-plane polar state is likely to be more favorable than the JT distortion due to the well-known polarization-strain coupling, and as mentioned earlier, the polar mode becomes softer since the frequency decreases as tensile epitaxial strain increases. The polar distortion in the STO layer is also an important influence. To show this, we fixed the STO layer in a nonpolar structure for 3% strain, froze in the in-plane polar mode and JT distortion in the CrO_2 layer in turn, and relaxed. Distortions survive in both cases and the relaxed structure with JT distortion has lower energy, suggesting that the in-plane polar mode in the STO coupled differently to the in-plane polar mode and the JT mode in the SCO layer.

This insulating state also raises the possibility of controlling band gap by applied electric field. Given the SCO/STO superlattice in the insulating state, an in-plane electric field will change the atomic positions, and hence change the band gap, because the band gap is sensitive to the displacement of the Cr atom relative to the O atoms around it.

In summary, we have studied both the lattice and electronic structures of the ground state for the 1:1 SCO/STO superlattice. Distortions in SCO layers are established by the superlattice layering with STO. For tensile epitaxial strain, due to the in-plane polar distortion associated with nonzero Cr displacements, the $d^1_{xy}d^1_{yz}d^0_{xz}$ orbital ordering can be formed and the band gap is therefore induced. The polar distortion induced metal-insulator transition can be used to engineer the SCO band structures near the Fermi level. Our study sheds light on a new way to control electronic band structures and approach the metal-insulator transition.

We acknowledge helpful discussions with K. Garrity, D. R. Hamann, H. Huang, S. Y. Park, D. Vanderbilt and H. Zhang. First-principles calculations are performed on the Rutgers University Parallel Computer (RUPC) cluster and the Center for Functional Nanomaterials (CFN) cluster at Brookhaven National Lab. This work is supported by NSF DMR-1334428, ONR N00014-11-1-0665, and ONR N00014-11-1-0666.

[1] M. Imada, A. Fujimori, and Y. Tokura, Rev. Mod. Phys. **70**, 1039 (1998).
[2] T. Hashimoto, S. Ishibashi, and K. Terakura, Phys. Rev. B **82**, 045124 (2010).
[3] J. H. Lee, K. T. Delaney, E. Bousquet, N. A. Spaldin, and K. M. Rabe, Phys. Rev. B **88**, 174426 (2013).
[4] R. F. Berger, C. J. Fennie, and J. B. Neaton, Phys. Rev. Lett. **107**, 146804 (2011).
[5] F. Wang, I. Grinberg, and A. M. Rappe, Appl. Phys. Lett. **104**, 152903 (2014).
[6] H.-T. Kim, B.-G. Chae, D.-H. Youn, G. Kim, K.-Y. Kang, S.-J. Lee, K. Kim, and Y.-S. Lim, Appl. Phys. Lett. **86**, 242101 (2005).
[7] Z. Yang, C. Ko, and S. Ramanathan, Ann. Rev. Mater. Res. **41**, 337 (2011).
[8] B. Chamberland, Solid State Commun. **5**, 663 (1967).
[9] A. C. Komarek, T. Möller, M. Isobe, Y. Drees, H. Ulbrich, M. Azuma, M. T. Fernández-Díaz, A. Senyshyn, M. Hoelzel, G. André, Y. Ueda, M. Grüninger, and M. Braden, Phys. Rev. B **84**, 125114 (2011).
[10] L. Ortega-San-Martin, A. J. Williams, J. Rodgers, J. P. Attfield, G. Heymann, and H. Huppertz, Phys. Rev. Lett. **99**, 255701 (2007).
[11] K.-W. Lee and W. E. Pickett, Phys. Rev. B **80**, 125133 (2009).
[12] Z.-L. Zhu, J.-H. Gu, Y. Jia, and X. Hu, Physica B **407**, 1990 (2012).
[13] K. Gupta, P. Mahadevan, P. Mavropoulos, and M. Ležaić, Phys. Rev. Lett. **111**, 077601 (2013).
[14] J.-S. Zhou, C.-Q. Jin, Y.-W. Long, L.-X. Yang, and J. B. Goodenough, Phys. Rev. Lett. **96**, 046408 (2006).
[15] J. M. Rondinelli and N. A. Spaldin, Phys. Rev. B **81**, 085109 (2010).
[16] M. Verissimo-Alves, P. García-Fernández, D. I. Bilc, P. Ghosez, and J. Junquera, Phys. Rev. Lett. **108**, 107003 (2012).
[17] G. Song and W. Zhang, Sci. Rep. **4** (2014).
[18] A. Antons, J. B. Neaton, K. M. Rabe, and D. Vanderbilt, Phys. Rev. B **71**, 024102 (2005).
[19] O. Diéguez, K. M. Rabe, and D. Vanderbilt, Phys. Rev. B **72**, 144101 (2005).
[20] Y. Zhou and K. M. Rabe, Phys. Rev. B **89**, 214108

(2014).
[21] J. P. Perdew and A. Zunger, Phys. Rev. B **23**, 5048 (1981).
[22] D. M. Ceperley and B. J. Alder, Phys. Rev. Lett. **45**, 566 (1980).
[23] G. Kresse and J. Hafner, Phys. Rev. B **47**, 558 (1993).
[24] G. Kresse and J. Furthmüller, Phys. Rev. B **54**, 11169 (1996).
[25] S. L. Dudarev, G. A. Botton, S. Y. Savrasov, C. J. Humphreys, and A. P. Sutton, Phys. Rev. B **57**, 1505 (1998).
[26] J. H. Lee and K. M. Rabe, Phys. Rev. B **84**, 104440 (2011).
[27] As a precise measurement of the magnetic moment is not available for SrCrO3, we chose $U_{eff} = 1.5$ eV to give agreement for the measured value for the in-plane lattice constant. We note that we find that the occupation of the dxy orbital for relaxed structures to be close to one for $U_{eff} = 1.5$ eV; this agreement with neutron diffraction experiments is the criterion used for choice of U in Ref. 11 (PRB 80, 124133 (2009)), though the value of U obtained there is different.
[28] P. E. Blöchl, Phys. Rev. B **50**, 17953 (1994).
[29] G. Kresse and D. Joubert, Phys. Rev. B **59**, 1758 (1999).
[30] N. A. Pertsev, A. G. Zembilgotov, and A. K. Tagantsev, Phys. Rev. Lett. **80**, 1988 (1998).
[31] See the Supplementary materials for detailed low energy structures of epitaxially strained $SrCrO_3$ and $SrTiO_3$ which includes Ref[32–34].
[32] P. Ghosez, D. Desquesnes, X. Gonze, and K. M. Rabe, AIP Conf. Proc. **535**, 102 (2000).
[33] Y. L. Li, S. Choudhury, J. H. Haeni, M. D. Biegalski, A. Vasudevarao, A. Sharan, H. Z. Ma, J. Levy, V. Gopalan, S. Trolier-McKinstry, D. G. Schlom, Q. X. Jia, and L. Q. Chen, Phys. Rev. B **73**, 184112 (2006).
[34] R. A. Evarestov, E. Blokhin, D. Gryaznov, E. A. Kotomin, and J. Maier, Phys. Rev. B **83**, 134108 (2011).
[35] A. M. Glazer, Acta Crystallographica Section B **28**, 3384 (1972).